

Off-line and on-line optical monitoring of microalgal growth

Hugo-Enrique Lazcano-Hernandez¹, Gabriela Aguilar², Gabriela Dzul², Rodrigo Patiño^{Corresp., 2}, Javier Arellano-Verdejo^{Corresp. 3}

¹ Cátedras CONACYT-El Colegio de la Frontera Sur, Chetumal, Quintana Roo, México

² Departamento de Física Aplicada, Cinvestav Unidad Mérida, Mérida, Yucatán, México

³ Estación para la Recepción de Información Satelital ERIS-Chetumal, El Colegio de la Frontera Sur, Chetumal, Quintana Roo, México

Corresponding Authors: Rodrigo Patiño, Javier Arellano-Verdejo

Email address: rodrigo.patino@cinvestav.mx, javier.arellano@mail.ecosur.mx

The growth of *Chlamydomonas reinhardtii* microalgae cultures was successfully monitored, using classic off-line optical techniques (optical density and fluorescence) and on-line analysis of digital images. In this study, it is shown that the chlorophyll fluorescence ratio F_{685}/F_{740} has a linear correlation with the logarithmic concentration of microalgae. Moreover, with digital images, the biomass concentration was correlated with the luminosity of the images through an exponential equation and the length of penetration of a superluminescent blue beam ($\lambda=440$ nm) through an inversely proportional function. The outcomes of this study are useful to monitor both research and industrial microalgae cultures.

Off-line and on-line optical monitoring of microalgal growth

Hugo E. Lazcano-Hernandez¹, Gabriela Aguilar², Gabriela Dzul², Rodrigo Patiño², and Javier Arellano-Verdejo³

¹Cátedras CONACYT-El Colegio de la Frontera Sur, Chetumal, Quintana Roo, México

²Departamento de Física Aplicada, Cinvestav Unidad Mérida, Mérida, Yucatán, México

³El Colegio de la Frontera Sur, Estación para la Recepción de Información Satelital ERIS-Chetumal, Chetumal, Quintana Roo, México.

Corresponding author:

Javier Arellano-Verdejo, Rodrigo Patiño

Email address: javier.arellano@mail.ecosur.mx, rodrigo.patino@cinvestav.mx

ABSTRACT

The growth of *Chlamydomonas reinhardtii* microalgae cultures was successfully monitored, using classic off-line optical techniques (optical density and fluorescence) and on-line analysis of digital images. In this study, it is shown that the chlorophyll fluorescence ratio F_{685}/F_{740} has a linear correlation with the logarithmic concentration of microalgae. Moreover, with digital images, the biomass concentration was correlated with the luminosity of the images through an exponential equation and the length of penetration of a super luminescent blue beam ($\lambda=440$ nm) through an inversely proportional function. The outcomes of this study are useful to monitor both research and industrial microalgae cultures.

INTRODUCTION

Photosynthesis is a biophotonic mechanism by which green plants, cyanobacteria and algae transform a fraction of the solar energy to biochemical energy in order to produce their own food. This is the foundation of life on Earth. Photosynthesis occurs in the chloroplasts, which are cell organelles that contain photosynthetic pigments (chlorophyll a, chlorophyll b, carotenoids, etc.). They absorb light and use it to drive photosynthetic light reactions and associated electron transport reactions to reduce CO_2 and oxidize H_2O in the Calvin cycle (Allen, 1992). The net result of photosynthesis is the production of carbohydrates and the release of molecular oxygen to the atmosphere. Environmental factors such as temperature, irradiance, humidity and salinity are known to affect photosynthesis (Rym, 2012).

Microalgae cultivation has been widely studied due to microalgae's potential as a source of food, biofuel, and various bioactive compounds. These are useful for important processes such as the cleaning of residual waters, CO_2 capture, and H_2 synthesis. All these are valuable products, which contribute to the balance and growth of human activity on a global scale (Gupta et al., 2015). A wide review of on-line and off-line technologies to monitor physicochemical and biological parameters of microalgae was compiled by Havlik and co-workers (Havlik et al., 2016). There are several photobioreactor models to predict growth (Pulz, 2001; Carvalho et al., 2006; Xu et al., 2009). However, actual measurements are required to monitor and optimize the algae growth process. Disadvantages of sampling include the potential for contaminating the culture, disturbing the algae's physiological state or modifying the volume of the medium. Another challenge for real-time measurements is the wide range of concentrations encountered in microalgal cultures. The concentration routinely increases by up to three orders of magnitude and this prevents direct measurement by most analytical methods (Antal et al., 2019). Therefore, it is currently a challenge to implement non-invasive real-time methodologies for monitoring microalgal cultivation conditions and photosynthetic parameters (Antal et al., 2019).

Chlorophyll (Chl) molecules are organized into two different light systems called Photosystem I (*PSI*) and Photosystem II (*PSII*). Both are spatially separated in the chloroplasts' thylakoid membranes (Breijo et al., 2006). Every photosystem contains an antenna light-harvesting complex (*LHC*) and central *Chl*

46 molecules. The photosystems differ from each other in their proportions of *Chl a*, *Chl b*, their reaction
47 centers' characteristics, and the electron carriers involved in their processes. In *PSI*, the reactive center
48 is called *P700* and is formed by two *Chl a* molecules that are attached to each other. *PSII* also contains
49 a reactive center called *P680* which is formed by two attached *Chl a* molecules. The nomenclature is
50 associated with the maximum wavelength (λ) absorption of both *PSI* and *PSII*: $\lambda=700$ nm and $\lambda=680$
51 nm, respectively (Gouveia-Neto et al., 2011). The maximum fluorescence wavelength may vary according
52 to the origin and kind of *Chl*, the culture medium, the environmental conditions, and the measurement
53 equipment. For example, at room temperature *Chl a* fluorescence around $\lambda=685$ nm is largely emitted
54 by *PSII* antenna, and fluorescence around $\lambda=740$ nm is emitted by *PSI* antenna (Krause and Weis,
55 1984; Roháček et al., 2008; Gouveia-Neto et al., 2011). In the fluorescence emission spectra of healthy,
56 suspension-diluted thylakoid membranes or isolated chloroplasts, a sharp peak around $\lambda=685$ nm with a
57 broad shoulder at about $\lambda=740$ nm has been observed (Krause and Weis, 1991). Although isolated *Chl b*
58 dissolved in an organic solvent exhibits fluorescence, this does not happen with *in vivo* cultures because
59 the excitation energy is transferred completely to *Chl a* (Gouveia-Neto et al., 2011).

60 The main function of the *LHC* is to transfer excitation energy to the photosynthetic reaction centers,
61 where photochemical reactions take place, however, a part of the absorbed light energy is dissipated
62 as heat or emitted as fluorescence (Misra et al., 2012). In other words, to return to the ground state,
63 the excited *Chl* molecule undergoes one of three processes. These include (i) driving photochemical
64 reactions (photosynthesis), (ii) dissipating as heat (thermal de-excitation), or (iii) being re-emitted as
65 light (fluorescence). These processes occur in competition so that any increase in the efficiency of one
66 will result in a decrease in the yield of the other two. *Chl* fluorescence is an intrinsic signal emitted
67 by plants, algae and cyanobacteria that can be employed to monitor their physiological state, including
68 changes in the photosynthetic apparatus, developmental processes, state of health, stress events and
69 stress tolerance. It can also be used to detect diseases or nutrient deficiency (Gouveia-Neto et al., 2011;
70 Hák et al., 1990). Hence, by measuring the yield of *Chl* fluorescence, information about changes in the
71 efficiency of photosynthesis and heat dissipation can be obtained (Maxwell and Johnson, 2000; Krause
72 and Weis, 1984). Therefore, the simultaneous measuring of *Chl* fluorescence at $\lambda=685$ nm (F_{685}) and
73 $\lambda=740$ nm (F_{740}) allows for an approximate determination of *Chl* content in a non-destructive way using
74 the *Chl* ratio (F_{685}/F_{740}) (Hák et al., 1990).

75 Depending on the type of study and the suitability of the photosynthetic system, different fluores-
76 cence techniques have been used (Mauzerall, 1972; Olson et al., 1996; Kolber et al., 1998; Gorbunov
77 and Falkowski, 2004; Johnson, 2004; Chekalyuk and Hafez, 2008). At present, two *Chl* fluorescence
78 approaches are used to monitor photosynthetic efficiency in microalgae mass cultures. These are rapid
79 fluorescence induction and the saturation-pulse method (Masojídek et al., 2011), which are well known
80 successful methods. Regarding outdoor algae cultures, specific fluorimeters have been used. The pulse
81 amplitude modulation (*PAM*) fluorimeter provides rapid light responses curves of *PSII*. The dual *PAM*
82 fluorimeter estimates *PSI* and *PSII* yields, and the Induction Kinetics fluorimeter measures fluorescence
83 induction curves (Sukenik et al., 2009; Kromkamp et al., 2009; Masojídek et al., 2010). However,
84 real-time non-invasive methodologies are still needed to monitor microalgae culture growth conditions.
85 Therefore, two room temperature fluorescence methods are proposed in this study in order to measure
86 *Chlamydomonas reinhardtii* (*C. reinhardtii*) culture growth. The first is an analytic off-line optical
87 technique and the second involves on-line digital image analysis. *C. reinhardtii* is considered one of the
88 most promising eukaryotic H_2 producers (Torzillo et al., 2015), which is why its study is relevant. The
89 methodologies proposed here were applied to study the growth of *C. reinhardtii*. It is possible to apply
90 the proposed methods to other species. However, results will vary according to specific strain features, the
91 culture medium, PBR geometry, light sources, and temperature. However, the methods are simple and
92 easy to implement and assess.

93 1 MATERIALS AND METHODS

94 This project aimed at identifying alternative optical techniques for monitoring microalgal growth. Our hy-
95 potheses were that *C. reinhardtii* cell culture concentration correlates with (1) the off-line *Chl* fluorescence
96 ratio F_{685}/F_{740} and (2) the on-line image culture color, and (3) the on-line image culture fluorescence.

1.1 Microalgae cultures

C. reinhardtii (CC-124) microalgae were purchased from the Chlamydomonas Resource Center (USA) and grown photoautotrophically in a Sueoka medium (Sueoka, 1960). Growth conditions included continuous air bubbling ($1VVM = 1L - air/min/L - medium$) under controlled room temperature conditions (298 ± 2) K. Experiments were performed in two series. The first series was conducted for the off-line optical density and fluorimetry measurements (Experiments A and B). The second series was conducted for the on-line techniques that use digital images (Experiments 1 to 5). A portable spectrometer (*StellarNet, EPP2000*) was used to measure the optical density, fluorescence and color of the microalgae cultures, with a detection range between 200 and 850 nm. Spectrawiz software (*StellarNet, OS V5.0 ©2011*) was used for spectrometer measurements. In order to monitor the cell growth, optical density (OD) measurements at $\lambda = 640$ nm were taken. Each measurement was repeated three times for every sample. In a previous study, the dry weight of the microalgae was correlated with the OD of the algae cultures (del Campo et al., 2014). Limitations of the OD technique as well as its applications to other species and another culture medium were discussed by Griffiths and co-workers (Griffiths et al., 2011).

For the off-line experiments, three 1-L Roux culture bottles were used, each with 0.9L of algae culture, with continuous air bubbling ($1L/min$), under controlled room temperature conditions (Figure 1a). The cultures were illuminated continuously with two fluorescent lamps (Philips, *F20T12/D20W*). To assess the microalgae growth kinetics, three samples of 3mL each were taken from every bottle every 12 hours for five days. Additionally, a final control measurement was taken on the seventh day. Triplicate OD and fluorescence measurements were taken for every sample. Two experiments were performed with the only difference being the initial microalgae concentration (x_0). These were labeled as Experiment A ($x_0 = 34 \pm 2mg/L$), and Experiment B ($x_0 = 42 \pm 2mg/L$). In summary, a total of 270 measurements were made for every off-line experiment. Therefore, the number of measurements provided statistical significance to this study.

For the on-line experiments, a 3-L column photo-bio-reactor (*PBR*) was used (Figure 1b). A transparent acrylic tube with a thickness of 25 mm and an inner diameter of 95 mm was used to build the 95-cm length *PBR*. Four fluorescent lamps (Tecno Lite, *T46500K20W*) were used to illuminate the center of the column with around $100 \mu\text{mol photons } m^{-2}s^{-1}$. To avoid external light, the *PBR* was placed inside a dark cabin. Five experiments were performed, during the five days of sampling. These included three experiments with continuous illumination (Experiments 1, 2, and 3), and two experiments with 12-h light/12-h dark cycles (Experiments 4 and 5). Both off-line samples and digital images were taken every 6 or 12 h. A webcam (*Logitech, Carl Zeiss Tessar HD 1080 p*) connected to a PC was used to capture the *PBR* digital images. For the color analysis, the images were captured with two fluorescent lamps located behind the *PBR*. These were turned on while the other two lamps remained turned off. For the fluorescent images, the pictures were captured in darkness and the culture only was illuminated with a blue beam from a super luminescent diode (maximal wavelength of 440 nm) and a light filter (*LSR-GARD ARGON, model 2204*) with a protection range within 190-520 nm. In order to measure fluorescence after a dark-adapted period, at least 15 min of darkness was provided before fluorescent stimulation. The images were analyzed in a LCD screen with an Integrating cube (*StellarNet, IC2*) and the portable spectrometer. The International Commission on Illumination (CIE LAB) scale was used for color measurements. To achieve a homogeneous representation of the color of every image, five measurements were taken from different regions of the *PBR*.

1.2 Fluorescence cabin

The experimental system to measure fluorescence was composed of two main parts: a fluorescence cabin and the portable spectrometer. Based on the spectrometer, the fluorescence cabin was designed, manufactured, and coupled to the system using an optical fiber (*StellarNet, F400*). Through this fiber, light was guided from the sample cuvette to the spectrometer detector. The fluorescence cabin configuration is shown in Figure 2a. The main components are a dark cabin, a cylindrical (14 mm i.d.) glass sample cuvette (4 mL), six light emission diodes (LED), feed and switching electronic circuits, an AC/DC electric current converter (output 5.4 V), and a multi-modal optical fiber connector. The dark cabin is a space where light does not come in from external sources. Inside the dark cabin, a base was used to fix the cuvette in a normal position (at 90 degrees) relative to the floor. Parallel to the floor, as exciting radiation, six LEDs were placed (Stereon, Ultra Blue), three to the right side of the sample cuvette and three to the left. This configuration ensured homogeneous illumination conditions. In Figure 2b, the spectrum of the

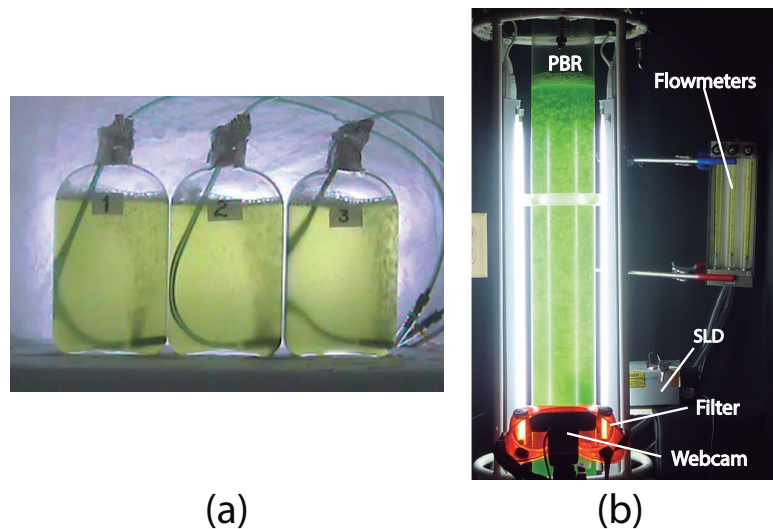


Figure 1. (a) The three Roux bottles for the off-line experiments (A and B), and (b) the column photo-bio-reactor (PBR) for the on-line experiments (1-5), Super Luminescent Diode (SLD); see Materials and Methods.

151 six LEDs is shown, with a maximum wavelength emission at around $\lambda=464$ nm, luminosity of 7 cd and
 152 400 mW as maximum power.

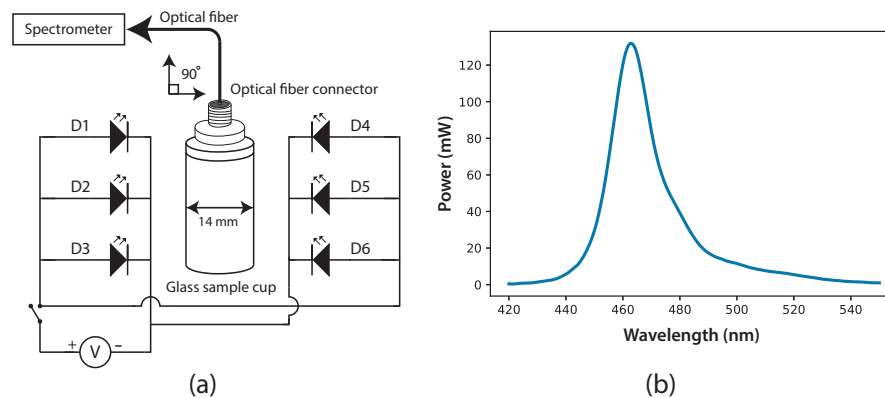


Figure 2. (a) Fluorescence cabin diagram, with optical fiber connector and glass sample cuvette; six Ultra Blue LEDs were installed as exciting source. (b) Spectrum of the exciting radiation source (Ultra Blue LEDs, $\lambda_{\text{max}} = 464$ nm).

153 To improve the quality of fluorescence measurement, the optical fiber was positioned on top of the
 154 glass sample cuvette, at 90° relative to the LEDs' radiation. Traditionally, fluorescence is measured
 155 through the sample cuvette wall. Instead of that, fluorescence measurements were taken at the uncovered
 156 top of the cuvette, thus reducing losses from reflection and refraction in the interface of the cuvette. The
 157 cuvette used for the samples was a 4-mL glass cylinder, but with this fluorescence system, the material
 158 and the geometry of the cuvette are not important. Light information was processed and digitalized by
 159 the spectrometer SpectraWiz software. Before measurements, the reference blank was defined by setting
 160 the spectrometer with the Sueoka medium; then, the fluorescence measurement was performed on the
 161 microalgae sample. The direct fluorescence of *C. reinhardtii* culture samples at room temperature was
 162 measured successfully for seven days with this experimental setup. The ratio of fluorescence intensity
 163 between $\lambda=685$ and $\lambda=740$ nm was calculated.

1.3 The F_{685}/F_{740} fluorescence ratio

At low *Chl* concentrations, fluorescence emissions increase with increasing amounts of *Chl*. At higher concentrations, the increase of fluorescence with the increment of *Chl* is mainly detected around 740 nm. For in vivo cultures, fluorescence emission at 740 nm is favored and fluorescence emission at 685 nm is not favored. This is due to the following factors: (i) the re-absorption of photons from the fluorescence emitted by neighboring molecules, (ii) light interference between the short (685 nm) and long wavelengths (740 nm), and (iii) the increment of *Chl* (the new *Chl* molecules preferentially absorb energy at 685 nm) (Gouveia-Neto et al., 2011).

There is a good inverse correlation between photochemistry and *Chl* fluorescence. The ratio of fluorescence intensity between maximal wavelengths (F_{685}/F_{740}) is influenced by photosynthetic activity. In mature microalgae cultures, the chloroplast structure, CO_2 uptake rate, carbon metabolism, etc., are better than in the younger cells. Higher F_{685}/F_{740} values signal young cultures or cultures with a not developing photosynthetic apparatus. Low values of this rate indicate mature cultures with a fully developed photosynthetic apparatus. In other words, the decrement in F_{685}/F_{740} values is indicative of increased photosynthetic activity. Measured through induction fluorescence, F_{685}/F_{740} exhibits a curvilinear relationship with cell concentration (x). This relationship can be successfully expressed by equation 1, where c and d are constants (Hák et al., 1990):

$$\frac{F_{685}}{F_{740}} = cx^{-d} \quad (1)$$

This technique has been applied to all kinds of leaves, chloroplast suspensions and acetone extracts of photosynthetic pigments. This study demonstrated that this technique is also applicable to microalgae cultures.

2 RESULTS AND DISCUSSION

2.1 Microbial growth

It has been established that the Gompertz model represents *C. reinhardtii* growth better than the classical Monod model (del Campo et al., 2014). Actually, the Monod and Gompertz models can be seen as particular cases of a more universal growth model (Castorina et al., 2006). For the experiments in the Roux bottles (A and B), as well as in the *PBR* (1-5), the Gompertz specific growth rate is reported in Table 1. For the *PBR* experiments, it was possible to observe that the Gompertz model is best fitted when the light regime is continuous (see R^2 for experiments 1-3) than when light/dark cycles are performed (experiments 4-5). Moreover, the specific growth rate is favored when the *PBR* is used. This stands in contrast to the cultures in the Roux bottles.

2.2 Fluorescence measurements

Variations in fluorescence intensity were successfully measured according to the increment in *C. reinhardtii* concentration. Some selected spectra are shown in Figure 3 for experiment A. The fluorescence dataset for experiments A and B are shown in supplementary material file (S1). In all cases, *Chl* fluorescence exhibits a peak around $\lambda=685$ nm and a broad shoulder around $\lambda=740$ nm. This is a general observation at room temperature for *Chl a* (Gouveia-Neto et al., 2011; Krause and Weis, 1984). The fluorescence around $\lambda=685$ nm is attributed to the *PSII* antenna, and the fluorescence around $\lambda=740$ nm is due to the *PSI* antenna (Gouveia-Neto et al., 2011). The fluorescence signal/noise ratio in the measurements was around 7 at $\lambda=740$ nm and 14 at $\lambda=685$ nm.

In Figure 4, fluorescence evolution at $\lambda=685$ nm and at $\lambda=740$ nm is shown for all bottles of experiments A. The plots include trend lines. In both experiments A and B, the maximum fluorescence intensity at $\lambda=685$ nm occurred between 48 and 60 hours. After that time, fluorescence decreased. Regarding fluorescence at $\lambda=740$ nm, in Experiment A, the maximum value occurred at 72 hours in all cultures. In Experiment B, the maximum value happened between 96 and 108 hours. For both experiments, the maximum fluorescence at $\lambda=685$ nm occurred before than at $\lambda=740$ nm. Maximum fluorescence at $\lambda=740$ nm occurred at the highest algae concentrations. In general, the results are consistent with those described in the literature for fluorescence in plants (Gouveia-Neto et al., 2011). Namely, at low *Chl* concentrations, fluorescence emissions increase with increasing *Chl* concentration. At higher

Reactor	Experiments	$\mu(\text{day}^{-1})$	R^2
Roux bottles	AI	0.5472	0.9981
	AII	0.5856	0.9989
	AIII	0.5424	0.9889
		0.56 ± 0.02	
	BI	0.3360	0.9843
	BII	0.4032	0.9965
PBR		0.3696	0.9944
		0.37 ± 0.03	
	1	0.7824	0.9954
	2	0.6720	0.9771
	3	0.6192	0.9656
		0.69 ± 0.08	
	4	0.3384	0.9180
	5	0.4776	0.9312
		0.41 ± 0.10	

Table 1. The Gompertz specific growth rate of microalgae in seven experiments, with the corresponding correlation values. The mean value and the standard deviation are reported for the cultures with continuous illumination (experiments A and B in the Roux bottles, and 1, 2, and 3 in the PBR) and with light/dark cycles (experiments 4 and 5 in the PBR).

212 concentrations, the increase of fluorescence with the increment of *Chl* was detected only around $\lambda=740$
213 nm.

214 Regarding the F_{685}/F_{740} ratio, it was possible to observe a similar behavior in every culture of both
215 experiments, regardless of the initial concentration. For that reason, Figure 5 shows the average of the
216 three cultures for each of the two experiments over five days, and a final measurement on the seventh
217 day. As time went by, the F_{685}/F_{740} fluorescence ratio decreased, and that means that the photosynthetic
218 processes were improved. The same trend has been reported for green leaves in plants, as stated in
219 equation 1 (Hák et al., 1990).

220 Based on the information in Figure 5, and considering the data of 168 hours as the minimum possible
221 value (aged cultures), we figured that cultures in both experiments reached around 70% of maturity at 96
222 hours. Therefore, every culture evolved successfully, which means that the conditions are appropriate
223 to grow the microalgae and keep them in a good state of health. In addition, the cultures that reached
224 the lowest F_{685}/F_{740} values, that is, the highest photosynthetic activity, were those of Experiment A,
225 which started with the lowest initial concentration. Moreover, after 72 hours, these values did not change
226 significantly. This is the moment when illumination may not be enough for the culture because cell
227 concentration reduces the passage of light. Finally, equation 2 expresses a very useful linear correlation
228 between the logarithmic concentration of microalgae and the F_{685}/F_{740} ratio through time (Figure 6):

$$\ln\left(\frac{x}{x_0}\right) = 3.27 - 0.7084(F_{685}/F_{740}) \quad (2)$$

229 2.3 Digital images

230 When the PBR was used, digital images of the cultures were taken to monitor the change in color and to
231 measure the penetration of a fluorescent beam during microalgae growth. Figure 7 shows a selection of
232 images illustrating a typical experiment. It was possible to observe that cultures get darker with time due
233 to the increase of biomass concentration in the PBR. This prevents the passage of light throughout the
234 reactor. For the fluorescence measurements, the flashes due to the blue super-luminescent diode were
235 filtered in order to measure only fluorescence light contribution. This contribution diminishes with time
236 due to a shadow effect produced by cells as the microalgae concentration gets denser.

237 CIELAB measurements include three values to characterize the color of a sample: L is the luminosity,
238 the parameter “a” represents colors from green to red, and the parameter “b” represents colors from

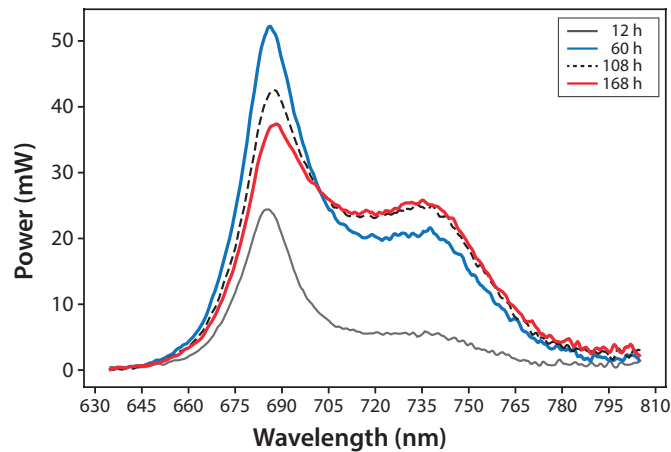


Figure 3. Microalgae fluorescence emission spectra ($298 \pm 2K$): evolution throughout seven days (168 h). Experiment A, $x_0 = (34 \pm 2)$ mg/L

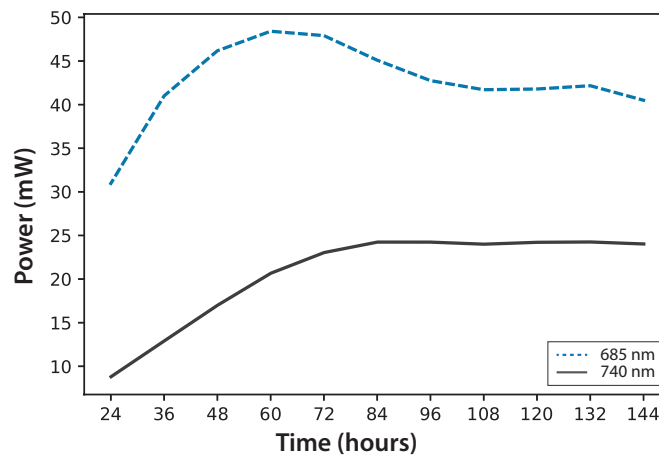


Figure 4. Experiment A: *C. reinhardtii* fluorescence evolution trend at $\lambda = 685$ nm and $\lambda = 740$ nm

239 blue to yellow. Both parameters “a” and “b” remained almost constant throughout the experiment
 240 during microalgae growth. This means that, technically, color does not change. This is expected since
 241 the photosynthetic pigments are always the same. In fact, luminosity is what diminishes importantly
 242 during cell growth since cells deflect or shadow light sources. In Figure 8, it is possible to observe the
 243 logarithmic correlation between microalgae concentration x , and luminosity L for experiments 1-3. For
 244 these experiments, equation 3 is proposed to get x from on-line measurements of L from digital images:

$$\ln\left(\frac{x}{x_0}\right) = (1.6 \pm 0.2) - (0.44 \pm 0.04)(L/W) \quad (3)$$

245 In this equation, the intercept and the slope values are presented as the mean and the corresponding
 246 standard deviation of the individual correlations in the three experiments (see Figure 8). However, this
 247 same correlation was not observed in experiments 4-5, where light/dark cycles were performed (Figure 9).
 248 A calculation of the correlations between the values of the three experiments confirms that the experiments
 249 are reproducible, which gives confidence to the study. Table 2 shows the $L(W)$ and Table 3 shows the
 250 correlation between $\ln(x/x_0)$ values.

251 Finally, the fluorescence beam penetration was characterized as an image changing with time. Both the
 252 beam surface area (data not shown) and penetration distance were used to monitor these changes. Similar
 253 results were obtained when comparing the cell concentration with the changes in the fluorescent images;
 254 therefore, only the distance beam penetration was used since its measurement is much simpler than that

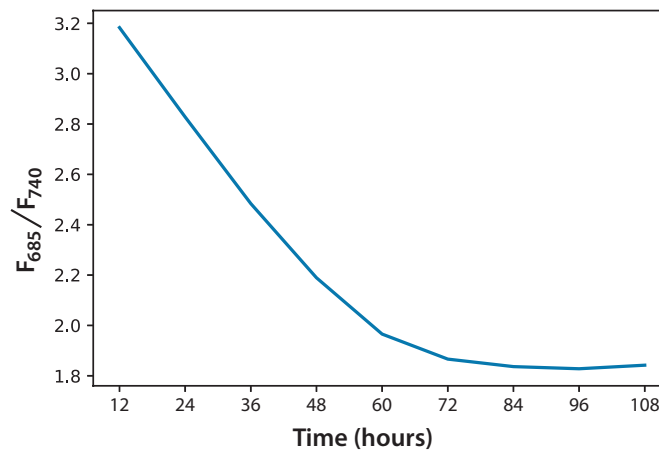


Figure 5. Fluorescence ratio (F_{685}/F_{740}) trend for *C. reinhardtii* for all experiments.

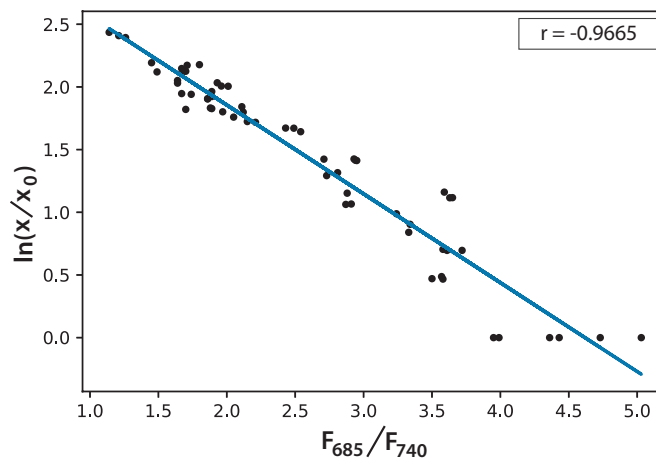


Figure 6. Linear correlation for the logarithmic microalgae concentration and the fluorescence ratio F_{685}/F_{740} ($r = -0.966578$)

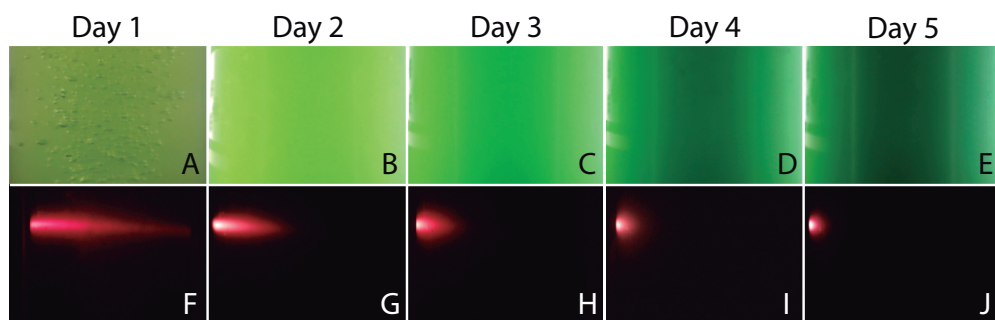


Figure 7. Representative images of the PBR captured every day during an experiment. Color assessment (Figures 7A-7E) and Fluorescent beam penetration (Figures 7F-7J).

255 of the surface area. In Figure 10, it is possible to observe the correlation of this distance measured for the
 256 fluorescent beam penetration with the inverse of the OD. As stated before, the OD is already related with
 257 the biomass concentration (del Campo et al., 2014). It is important to notice that the linear correlations
 258 were obtained for all experiments, with equation 4 proposed to calculate the OD of the culture directly
 259 from the on-line measure of the beam penetration:

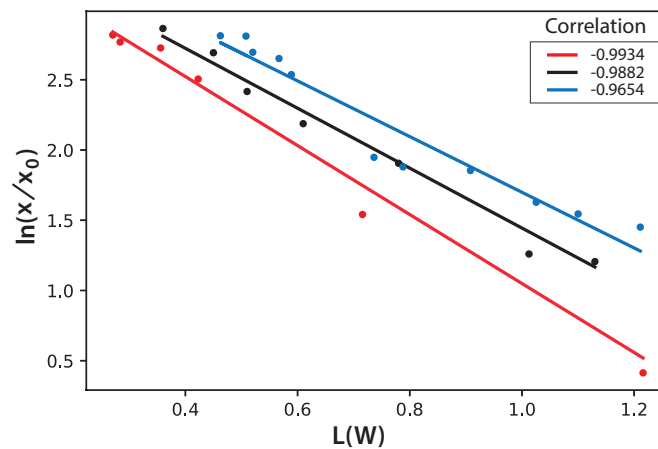


Figure 8. Logarithmic dependence of cell concentration with the luminosity (L) value in the CIELAB scale of colors, for the PBR experiments with continuous illumination. The colors correspond to experimental values: black (exp. 1), red (exp. 2), and blue (exp. 3); the lines correspond to the mean-squares correlations

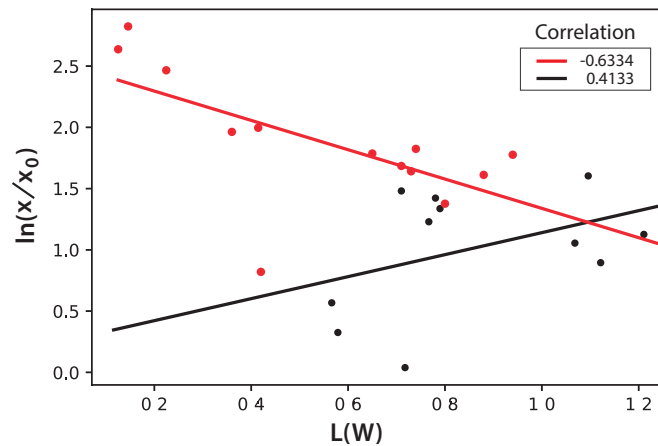


Figure 9. Logarithmic dependence of cell concentration with the luminosity (L) value in the CIELAB scale of colors, for the PBR experiments with light/dark cycles. The colors correspond to experimental values: black (exp. 4), red (exp. 5); the lines correspond to the mean-squares correlations

	E1	E2	E3
E1	1.000000	0.963332	0.942350
E2	0.963332	1.000000	0.973427
E3	0.942350	0.973427	1.000000

Table 2. $L(W)$ Correlation

	E1	E2	E3
E1	1.000000	0.973283	0.948333
E2	0.973283	1.000000	0.985426
E3	0.948333	0.985426	1.000000

Table 3. $\ln(x/x_0)$ Correlation

$$OD = \frac{1}{\text{beam penetration / cm}} \quad (4)$$

260 This simple equation is proposed since the values for the mean and the corresponding standard
 261 deviation for the intercept and the slope in the individual linear correlations for the five experiments are
 262 (0.0 ± 0.5) and $(1.0 \pm 0.1) \text{cm}^{-1}$ respectively.

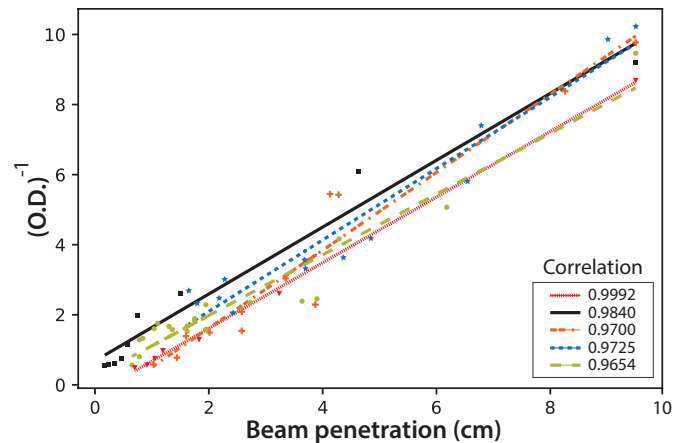


Figure 10. The inverse of microalgae culture optical density (OD), as a function of the fluorescent beam penetration in the PBR. The colors correspond to the following experimental values: red dash line (exp. 1), black (exp. 2), orange dotted line (exp. 3), blue dotted line (exp. 4) and light green dotted line (exp. 5); the lines correspond to the least-squares correlations.

263 3 CONCLUSIONS

264 The growth of *C. reinhardtii* cultures was successfully monitored through off-line and on-line optical
 265 techniques at an affordable cost. It was confirmed that, as evidenced in green plants, the maximum
 266 fluorescence around $\lambda=685$ nm occurs before that happening at $\lambda=740$ nm. The maximum fluorescence
 267 at $\lambda=740$ nm occurs at a higher concentration, compared to what is needed at $\lambda=685$ nm. Once the
 268 maximum fluorescence at $\lambda=685$ nm has been reached, it decreases before and at a faster rate than the
 269 fluorescence at $\lambda=740$ nm. Although the F_{685}/F_{740} fluorescence ratio is a well-known method, here it was
 270 demonstrated for the first time for *C. reinhardtii* cultures. A very useful linear correlation occurs between
 271 the logarithmic concentration of *C. reinhardtii* and the F_{685}/F_{740} ratio through time.

272 Moreover, the on-line analysis of digital images was also shown to be useful to monitor *C. reinhardtii*
 273 growth. The luminosity measurements in the CIELAB scale were linearly correlated with the microbial
 274 concentration for cultures under continuous illumination. However, for the cultures in a light/dark regime,
 275 this correlation was not found. Nevertheless, for the fluorescent beam penetration images, both the distance
 276 and the surface captured for the beam were linearly correlated with optical density and, consequently, with
 277 the microalgae culture density for all the illumination regimes. Indeed, a simple reciprocal equation can
 278 be used to calculate optical density as the inverse of the measured distance of beam penetration ($\lambda=440$
 279 nm).

280 The on-line techniques proposed here are very practical to study both research and industrial microal-
 281 gae cultures. As a future study, in the case of having multispectral remote sensing reflectances both at 685
 282 nm and 740 nm, and with the contribution of field measurements for calibration, it would be feasible to
 283 use equation 2 and regression models between the logarithmic concentration of microalgae and remote
 284 sensing data to estimate the concentration of Chlorophyll a in wide water areas.

285 ACKNOWLEDGMENTS

286 Hugo Lazcano thanks CONACyT for his postdoctoral fellowship and for the support provided through
 287 the “Cátedras-CONACYT” program (project 526). The authors are grateful to the editor and reviewers
 288 for their contribution to improve this manuscript. We thank Moisés Perales for his help with editing the
 289 manuscript.

290 **FUNDING**

291 This research did not receive any specific grant from funding agencies in the public, commercial, or
292 not-for-profit sectors.

293 **REFERENCES**

- 294 Allen, J. F. (1992). How does protein phosphorylation regulate photosynthesis? *Trends in biochemical*
295 *sciences*, 17(1):12–17.
- 296 Antal, T., Konyukhov, I., Volgusheva, A., Plyusnina, T., Khruschev, S., Kukarskikh, G., Goryachev, S.,
297 and Rubin, A. (2019). Chlorophyll fluorescence induction and relaxation system for the continuous
298 monitoring of photosynthetic capacity in photobioreactors. *Physiologia plantarum*, 165(3):476–486.
- 299 Breijo, F. J. G., Caselles, J. R., and Siurana, P. S. (2006). *Introducción al funcionamiento de las plantas*.
300 Ed. Univ. Politéc. Valencia.
- 301 Carvalho, A. P., Meireles, L. A., and Malcata, F. X. (2006). Microalgal reactors: a review of enclosed
302 system designs and performances. *Biotechnology progress*, 22(6):1490–1506.
- 303 Castorina, P., Delsanto, P., and Guiot, C. (2006). Classification scheme for phenomenological universalities
304 in growth problems in physics and other sciences. *Physical review letters*, 96(18):188701.
- 305 Chekalyuk, A. and Hafez, M. (2008). Advanced laser fluorometry of natural aquatic environments.
306 *Limnology and Oceanography: Methods*, 6(11):591–609.
- 307 del Campo, J. S. M., Escalante, R., Robledo, D., and Patino, R. (2014). Hydrogen production by
308 *Chlamydomonas reinhardtii* under light-driven and sulfur-deprived conditions: using biomass grown
309 in outdoor photobioreactors at the Yucatan peninsula. *International journal of hydrogen energy*,
310 39(36):20950–20957.
- 311 Gorbunov, M. Y. and Falkowski, P. G. (2004). Fluorescence induction and relaxation (fire) technique and
312 instrumentation for monitoring photosynthetic processes and primary production in aquatic ecosystems.
313 In *Photosynthesis: Fundamental Aspects to Global Perspectives*—Proc. 13th International Congress of
314 *Photosynthesis, Montreal, Aug*, pages 1029–1031.
- 315 Gouveia-Neto, A. S., da Silva-Jr, E. A., Cunha, P. C., Oliveira-Filho, R. A., Silva, L. M., da Costa, E. B.,
316 Camara, T. J., and Willadino, L. G. (2011). Abiotic stress diagnosis via laser induced chlorophyll
317 fluorescence analysis in plants for biofuel. In *Biofuel Production—Recent Developments and Prospects*.
318 IntechOpen.
- 319 Griffiths, M. J., Garcin, C., van Hille, R. P., and Harrison, S. T. (2011). Interference by pigment in the
320 estimation of microalgal biomass concentration by optical density. *Journal of microbiological methods*,
321 85(2):119–123.
- 322 Gupta, P. L., Lee, S.-M., and Choi, H.-J. (2015). A mini review: photobioreactors for large scale algal
323 cultivation. *World Journal of Microbiology and Biotechnology*, 31(9):1409–1417.
- 324 Hák, R., Lichtenthaler, H., and Rinderle, U. (1990). Decrease of the chlorophyll fluorescence ratio
325 f_{690}/f_{730} during greening and development of leaves. *Radiation and environmental biophysics*,
326 29(4):329–336.
- 327 Havlik, I., Scheper, T., and Reardon, K. F. (2016). *Monitoring of Microalgal Processes*, pages 89–142.
328 Springer International Publishing, Cham.
- 329 Johnson, Z. I. (2004). Description and application of the background irradiance gradient-single turnover
330 fluorometer (big-stf). *Marine Ecology Progress Series*, 283:73–80.
- 331 Kolber, Z. S., Prášil, O., and Falkowski, P. G. (1998). Measurements of variable chlorophyll fluorescence
332 using fast repetition rate techniques: defining methodology and experimental protocols. *Biochimica et*
333 *Biophysica Acta (BBA)-Bioenergetics*, 1367(1-3):88–106.
- 334 Krause, G. and Weis, E. (1991). Chlorophyll fluorescence and photosynthesis: the basics. *Annual review*
335 *of plant biology*, 42(1):313–349.
- 336 Krause, G. H. and Weis, E. (1984). Chlorophyll fluorescence as a tool in plant physiology. *Photosynthesis*
337 *research*, 5(2):139–157.
- 338 Kromkamp, J. C., Beardall, J., Sukenik, A., Kopecký, J., Masojídek, J., Van Bergeijk, S., Gabai, S.,
339 Shaham, E., and Yamshon, A. (2009). Short-term variations in photosynthetic parameters of nan-
340 nochloropsis cultures grown in two types of outdoor mass cultivation systems. *Aquatic Microbial*
341 *Ecology*, 56(2-3):309–322.
- 342 Masojídek, J., Kopecký, J., Giannelli, L., and Torzillo, G. (2011). Productivity correlated to photobio-

- 343 chemical performance of chlorella mass cultures grown outdoors in thin-layer cascades. *Journal of*
344 *industrial microbiology & biotechnology*, 38(2):307–317.
- 345 Masojidek, J., Vonshak, A., and Torzillo, G. (2010). Chlorophyll fluorescence applications in microalgal
346 mass cultures. In *Chlorophyll a fluorescence in aquatic sciences: methods and applications*, pages
347 277–292. Springer.
- 348 Mauzerall, D. (1972). Light-induced fluorescence changes in chlorella, and the primary photoreactions
349 for the production of oxygen. *Proceedings of the National Academy of Sciences*, 69(6):1358–1362.
- 350 Maxwell, K. and Johnson, G. N. (2000). Chlorophyll fluorescence—a practical guide. *Journal of*
351 *experimental botany*, 51(345):659–668.
- 352 Misra, A. N., Misra, M., and Singh, R. (2012). Chlorophyll fluorescence in plant biology. In *Biophysics*.
353 IntechOpen.
- 354 Olson, R. J., Chekalyuk, A. M., and Sosik, H. M. (1996). Phytoplankton photosynthetic characteristics
355 from fluorescence induction assays of individual cells. *Limnology and oceanography*, 41(6):1253–1263.
- 356 Pulz, O. (2001). Photobioreactors: production systems for phototrophic microorganisms. *Applied*
357 *microbiology and biotechnology*, 57(3):287–293.
- 358 Roháček, K., Soukupová, J., and Barták, M. (2008). Chlorophyll fluorescence: a wonderful tool to study
359 plant physiology and plant stress. *Plant Cell Compartments-Selected Topics. Research Signpost, Kerala,*
360 *India*, pages 41–104.
- 361 Rym, B. D. (2012). Photosynthetic behavior of microalgae in response to environmental factors. In
362 *Applied Photosynthesis*. IntechOpen.
- 363 Sueoka, N. (1960). Mitotic replication of deoxyribonucleic acid in chlamydomonas reinhardi. *Proceedings*
364 *of the National Academy of Sciences of the United States of America*, 46(1):83.
- 365 Sukenik, A., Beardall, J., Kromkamp, J. C., Kopecký, J., Masojidek, J., van Bergeijk, S., Gabai, S.,
366 Shaham, E., and Yamshon, A. (2009). Photosynthetic performance of outdoor nanochloropsis mass
367 cultures under a wide range of environmental conditions. *Aquatic Microbial Ecology*, 56(2-3):297–308.
- 368 Torzillo, G., Scoma, A., Faraloni, C., and Giannelli, L. (2015). Advances in the biotechnology of
369 hydrogen production with the microalga chlamydomonas reinhardtii. *Critical reviews in biotechnology*,
370 35(4):485–496.
- 371 Xu, L., Weathers, P. J., Xiong, X.-R., and Liu, C.-Z. (2009). Microalgal bioreactors: challenges and
372 opportunities. *Engineering in Life Sciences*, 9(3):178–189.